THE JOURNAL OF PHYSICAL CHEMISTRY C

Article

pubs.acs.org/JPCC

Hydrogen Evolution from Pt Nanoparticles Covered p-Type CdS:Cu Photocathode in Scavenger-Free Electrolyte

Qiang Huang,[†,§] Quan Li,[†] and Xudong Xiao*[,†,‡]

[†]Department of Physics, The Chinese University of Hong Kong, Shatin, New Territory, Hong Kong, China

[‡]Shenzhen Institute of Advanced Technology, Chinese Academy of Science, Shenzhen, China

[§]Science and Technology on Surface Physics and Chemistry Laboratory, P.O. Box 718-35, Mianyang 621907, Sichuan, China

ABSTRACT: The photoelectrolysis of water to generate hydrogen by semiconductor photoelectrodes has been known to be a promising approach to utilize clean and sustainable solar energy. In this study, photocathode based on p-type CdS:Cu was successfully fabricated by the thermal evaporation process and photoelectrochemical investigations were carried out to determine its water photoelectrolysis potential. Cu doping concentration at 5.4% was found to be the optimal doping level and the bare CdS:Cu photocathode showed a large transient photocurrent as a result of the slow water reduction kinetics of the photoinduced electrons at the photoelectrode/electrolyte interface. The electrons accumulated at the interface and caused the photocathode to suffer from photodegradation during the stability test. After modifying the photocathode surface with the Pt nanoparticles to reduce the hydrogen evolving reaction overpotential, both the photocurrent and stability were enhanced. Hydrogen evolution from the CdS:Cu/Pt surface in the near neutral and scavenger-free electrolyte demonstrated for the first time the CdS with p-type conductivity was a feasible candidate for solar water splitting.

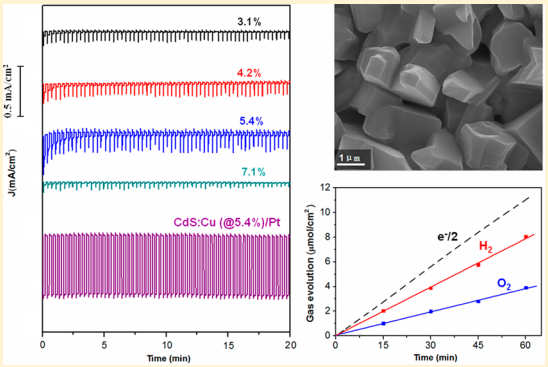

INTRODUCTION

Hydrogen is a promising energy carrier because it has a high gravimetric energy (143 MJ/kg) and is carbon free.[1] Among all the methods to produce hydrogen, direct photoreduction of water into hydrogen by semiconductor photoelectrodes has attracted great attention since the raw materials used are only water and sunlight, both of which are widely distributed.[2−4] Since the discovery by Fujishima and Honda, who used TiO_2 photoelectrode to demonstrate the solar water splitting in 1972, some metal oxides, such as TiO_2 and $SrTiO_3$, have been extensively investigated for their earth abundance and good stability in solution.[5,6] Unfortunately, their theoretical solar energy conversion efficiencies are quite low because of the large band gaps (i.e., 3.0−3.2 eV) which limit the sunlight absorption to the UV region.[7] As a result, materials responding to visible light, such as Si, InP, GaP, Fe_2O_3, WO_3, Cu_2O, and $GaInP_2$, have become more and more popular in developing practical water splitting cells.[2,8−15] Compared to them, CdS, with a direct band gap of 2.4 eV and appropriate valence/conduction energy band edges for water oxidation/reduction even after considering their respective overpotentials, as shown in Figure 1,[16−19] is a more promising candidate for water splitting without external bias (the overpotential required by water oxidation is much higher than that of water reduction). However, n-type CdS as a photoanode suffers significant photocorrosion due to its self-photooxidation at the photoelectrode/electrolyte interface by the photogenerated holes. Some scavengers, such as S^{2-} and SO_3^{2-}, were often required to prevent this photocorrosion by competing with CdS to capture the holes.[18,20] Although hydrogen gas was indeed generated

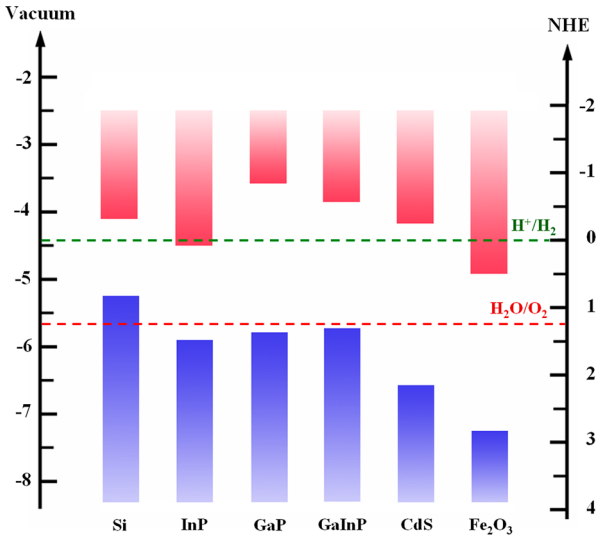

Figure 1. Overview of the energy band positions for several semiconductors and water oxidation/reduction states.[7,16,19]

Received: October 15, 2013
Revised: January 15, 2014
Published: January 15, 2014

   dx.doi.org/10.1021/jp410242e | J. Phys. Chem. C 2014, 118, 2306−2311

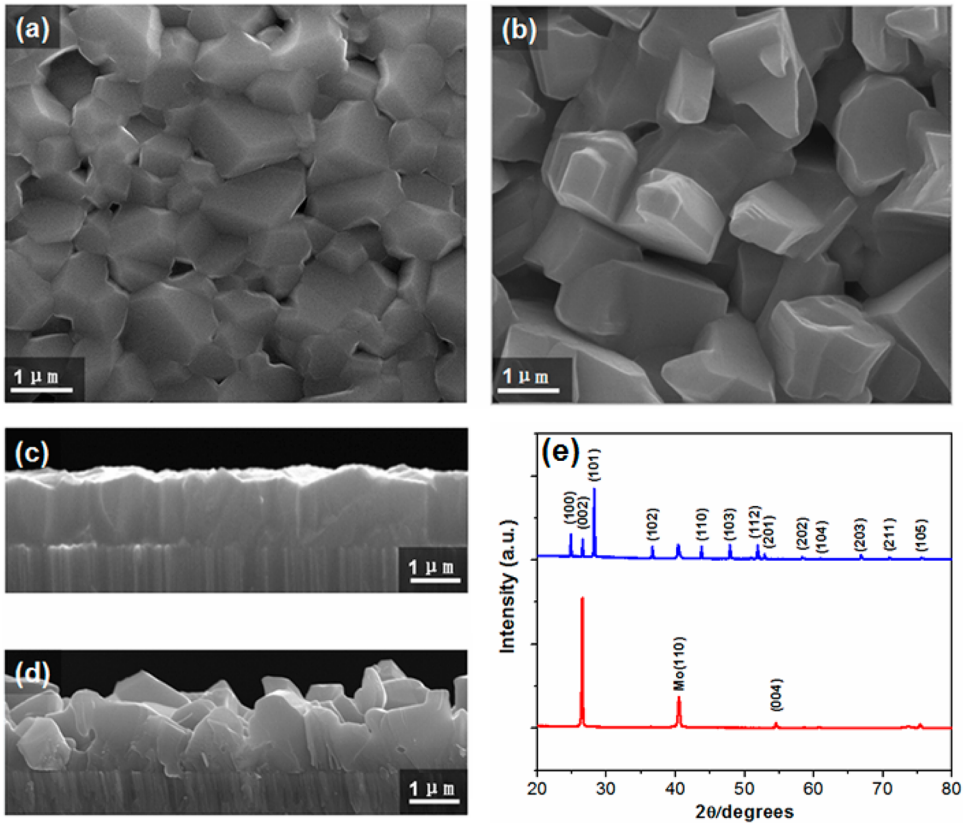

Figure 2. Structural characterization of n-CdS and CdS:Cu films on Mo back contact. SEM images of n-CdS (a, c) and CdS:Cu (@5.4%) (b, d). (e) XRD patterns of n-CdS (red line) and CdS:Cu (@5.4%) (blue line).

with this approach, it is not advantageous in the practical large-scale application as the energy required is not only the solar energy but also the chemical energy contained in the scavenger agents. Fortunately, the photocathodes based on p-type semiconductor materials were found to be cathodically protected from photooxidation.[2,17] Here, during the water photoelectrolysis process, the photon-excited electrons will migrate to the photocathode/electrolyte interface and the holes will transport to the counter electrode through external circuit. Thus, the p-type photocathode becomes responsible for the water reduction (H_2O/H_2) reaction involving the electrons and the more complex water oxidation (H_2O/O_2) reaction is transferred to the conventional metal counter electrode.[2,21] With the above advantages in band alignment and cathodic protection, p-type CdS deserves a systematic photoelectrolysis study. In the past, no effort was reported on the potential of p-type CdS in solar water splitting, possibly due to the inevitable self-compensation effect from intrinsic S vacancies (V_S) that serve as donor dopants.[22] In the case of the p-type CdS based photocathode, we should also consider the self-photoreduction, though much less significant than the self-photooxidation suffered by the n-type CdS photoanode, which results from the accumulation of photoexcited electrons at the photocathode/electrolyte interface. The accumulation of electrons caused by the slow water reduction kinetics of the photocathode surface could shift up the electron quasi-Fermi level to the reduction energy level to decompose CdS.[23]

Here, we report our successful preparation of the p-type CdS:Cu via thermal diffusion of Cu atoms during the growth of CdS thin film and our photoelectrochemical investigations to determine its water photoelectrolysis activity. Previously, group VA and IB elements have been used to dope CdS to achieve p-type conductivity.[24−26] In particular, doping Cu by thermal diffusion, laser ablation, or in situ chemical bath deposition were found to be effective tactics to fabricate p-type CdS.[27−29] Photovoltaic solar cells based on Cu-doped CdS (CdS:Cu), which was prepared by thermal diffusion of Cu into intrinsic CdS thin film via post vacuum annealing, have achieved an energy conversion efficiency of 8.5%.[30] We found for water photoelectrolysis that the optimal doping level is at 5.4% Cu concentration (Cu/Cd atomic ratio at %) and the modification of CdS:Cu surface with Pt cocatalyst, which presumably reduces the water reduction overpotential, can effectively enhance not only the photocurrent but also the stability. For the first time, we demonstrated hydrogen gas evolution from the CdS:Cu/Pt photocathode, revealing that the p-type CdS is a feasible candidate for water splitting and can overcome the shortcomings of n-type CdS. Considering the photoelectrolysis activity, photoelectrode stability, and the use of nearly neutral and scavenger-free electrolyte as a whole, the p-type CdS reported here is one of the best among all the photocathodes studied so far.

EXPERIMENTAL SECTION

Photoelectrode Preparation. Both the intrinsic and Cu-doped CdS thin films were prepared by thermal evaporation in a horizontal single zone tube furnace. The CdS powder (Aldrich, 99.995% purity) source was placed at the center of the furnace and the substrate was positioned about 30 cm away along the downstream direction. Mo film with a thickness of 1 μm on soda-lime glass, which was found to form ohmic contact with the sulfur-containing compounds such as $CuInS_2$ and

dx.doi.org/10.1021/jp410242e | J. Phys. Chem. C 2014, 118, 2306−2311

Cu(In,Ga)S_2 due to the formation of an ultrathin MoS_2 layer,[31,32] was used here as the back contact of the CdS photoelectrode. For preparation of the Cu-doped CdS, a Cu layer was deposited on top of the Mo layer and the incorporation of Cu atoms as acceptor centers into CdS was achieved during the CdS growth process through diffusion.[26,33] After the furnace chamber reached a pressure of 2×10^{-2} Torr by mechanical pumping, the temperature of the system was elevated to 750 °C at a rate of 20 deg/min. Argon gas, while maintaining a pressure of ~2.0 Torr, was sent through the system at a rate of 100 sccm to act as the carrier gas to transport the sublimated CdS vapor to the cooler substrate (380 °C) for deposition. Afterward, Pt serving as the cocatalyst for hydrogen evolution was deposited onto the CdS:Cu film by DC sputtering.

Characterizations. The morphology of the photoelectrode was imaged by SEM (Quanta 400, FEI) and the crystal structure was analyzed by X-ray diffractometry (Smart Lab, Rigaku). The charge carrier concentration and Hall mobility of CdS:Cu films with different Cu doping concentrations were measured with a Hall system (HL5500, Bio-Rad Microscience). The photoelectrochemical performance of the photoelectrode was evaluated with a standard electrochemical workstation (CHI660C, CH Instruments) in the three-electrode configuration. Here, a Pt wire was used as the counter electrode, an Ag/AgCl electrode in saturated KCl served as the reference electrode, and 1.0 M Na_2SO_4 solution at pH 9.0 was employed as the electrolyte. The light source was a 300-W Xe lamp equipped with a 400-nm long-pass filter (10LWF-400-B, Newport) and the light intensity was calibrated with a Si diode to simulate AM 1.5 illumination intensity (100 mW/cm^2). The linear sweep voltammetry was scanned at a rate of 10 mV/s and the photocurrent−time test under chopped light (light on/off cycles: 10 s) was carried out at a fixed potential of 0 V versus reversible hydrogen electrode (RHE). The hydrogen production measurement was carried out in a sealed Pyrex reaction cell, which was connected to a gas chromatograph with a thermal conductivity detector (TCD) and a 0.5 nm molecular sieve capillary column (GC 7900, Techcomp) via a gas circulation pump. The amount of charge passing through the photoelectrode and the amount of hydrogen gas produced was measured simultaneously to calculate the Faradic efficiency.

RESULTS AND DISCUSSION

With scanning electron microscopic (SEM) images, parts a and b of Figure 2 showed the surface morphology of the n-CdS and CdS:Cu films, respectively. It was found that the voids among different grains of CdS:Cu were much larger than those of the undoped one. Here, we used the CdS:Cu with 5.4% Cu as the representative for comparison with the n-CdS. The cross-sectional SEM image (Figure 2c,d) also confirmed the rougher surface of CdS:Cu and thus implied its larger surface-to-volume ratio. The larger surface area could in fact better facilitate the transfer of the photoinduced carriers from the photoelectrode to the electrolyte.[14,34−36] Comparing with the p-type CdS prepared by other methods such as the post vacuum annealing of Cu/CdS bilayers,[30] the high surface roughness reported here was obvious, indicating that the simultaneous CdS deposition and Cu diffusion not only simplifies the fabrication procedure but also produces photoelectrodes advantageously in the interest of water splitting. The X-ray diffraction (XRD) patterns displayed in Figure 2e confirmed that all the peaks of the n-CdS (blue line) and CdS:Cu (red line) corresponded to the CdS hexagonal structure. The intense peak of the n-CdS was assigned to (002), which indicated that the *c*-axis of the crystallites were generally oriented perpendicular to the substrate. In contrast, many more diffraction peaks arose in the CdS:Cu film, indicating the disordered nature of the crystallite orientations, which, associated with the surface roughening discussed above, were attributed to the simultaneous Cu incorporation.[26,27]

Figure 3a showed the absorption $(\alpha h\nu)^2$ versus photon energy $h\nu$ plots for the n-CdS and CdS:Cu (@5.4%) films. The

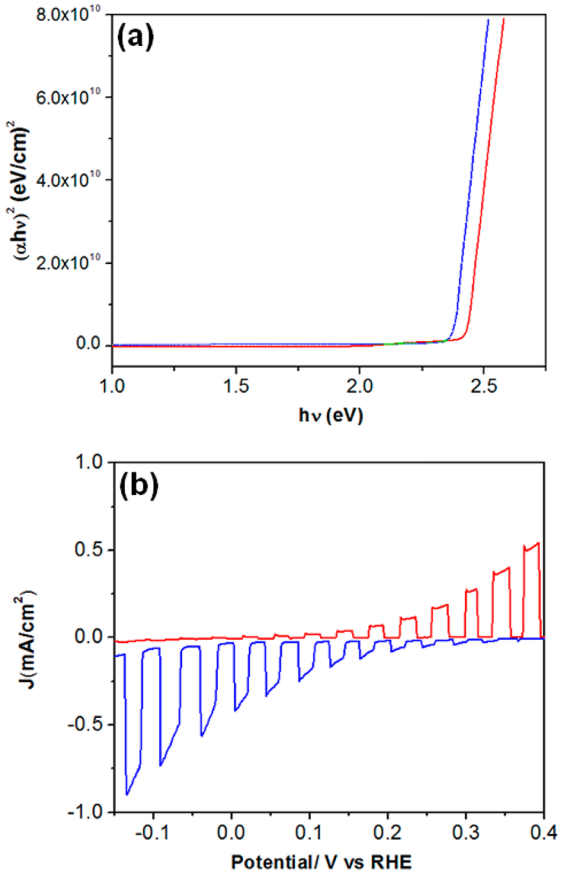

Figure 3. (a) $(\alpha h\nu)^2$ versus $h\nu$ plots of n-CdS (red line) and CdS:Cu (@5.4%) (blue line). (b) Current−potential curves of n-CdS (red line) and CdS:Cu (@5.4%) (blue line) under chopped simulated AM 1.5 light measured in 1.0 M Na_2SO_4 electrolyte at pH 9.

corresponding band gap value could be found by extrapolating the linear portions of the line to $(\alpha h\nu)^2 = 0$. Due to the substitution of Cu for Cd in the CdS lattice, the direct band gap E_g for CdS:Cu (@5.4%) was 2.37 eV, decreased from the value of 2.42 eV for n-CdS but in agreement with previous results.[37] Figure 3b showed the current−potential curves in the nearly neutral (pH 9) scavenger-free electrolyte under chopped simulated AM 1.5 light illumination. The anodic photocurrent of the n-CdS illuminated its n-type conductivity, and, in contrast, the cathodic photocurrent characteristic confirmed the p-type nature of CdS:Cu.[11] This result was consistent with the previous work which used the p-type CdS:Cu to form a p−n junction with the intrinsic n-type CdS in fabrication of photovoltaic solar cells and light emission diodes.[26,38,39]

Figure 4 showed the current−time curves of the CdS:Cu photocathodes with different Cu concentrations at 0 V versus RHE in 1.0 M Na_2SO_4 electrolyte at pH 9 under chopped

dx.doi.org/10.1021/jp410242e | J. Phys. Chem. C 2014, 118, 2306−2311

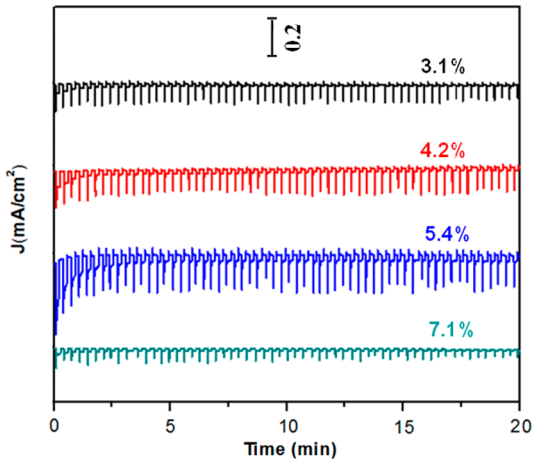

Figure 4. Current−time measurements for a number of CdS:Cu photocathodes with different Cu concentrations held at 0 V versus RHE in 1.0 M Na_2SO_4 electrolyte at pH 9 under chopped simulated AM 1.5 light. The insert is the 0.2 mA/cm^2 scale bar.

simulated AM 1.5 light. It is found that the photocathode with 5.4% Cu concentration was the optimal and had the best photoresponse. The electrical properties including carrier mobility and concentration of these films were analyzed by Hall measurements and the results were listed in Table 1. The

Table 1. Carrier Mobility and Concentration of Various CdS:Cu Films

Cu/Cd (%)	mobility (cm^2/V.s)	carrier concn (cm^{-3})
0	14.7	-6.4×10^{14}
3.1	4.9	$+4.7 \times 10^{17}$
4.2	4.2	$+6.8 \times 10^{18}$
5.4	3.9	$+1.7 \times 10^{19}$
7.1	0.14	$+2.3 \times 10^{19}$

positive sign of the carriers confirmed again the p-type nature of the CdS:Cu films at these doping levels. The carrier concentration was much lower than the Cu concentration. Taking the CdS:Cu (@5.4%) film as an example, the carrier concentration was only 1.7×10^{19}/cm^3 while the Cu concentration was 1.1×10^{21}/cm^3. This big difference was attributed to the self-compensation by native vacancies (such as the V_S donors), which were induced in the intrinsic n-type conductivity as shown by Figure 3b and Table 1 (negative sign of the carriers), and the insufficient ionizability of Cu_{Cd} dopants at room temperature as a result of the formed deep acceptors.[22,38] Woods and Champion suggested that the p-type conductivity of CdS:Cu might originate from the hopping conduction rather than from the impurity band conduction.[40] From Table 1, we found that the carrier mobility decreased after doping Cu atoms, and above 5.4% Cu concentration it suffered from a further accelerated reduction. The conflicting demand between high carrier concentration and high carrier mobility resulted in the optimal Cu doping level of 5.4%. The existence of optimal doping concentration was also reported by Liu et al. for the Zn-doped p-type GaP photocathode.[11]

The bare CdS:Cu photocathodes exhibited high transient photocurrents as shown in Figure 4, which were attributed to the accumulation of photoexcited electrons at the photocathode/electrolyte interface because of the slow water reduction kinetics.[11] With Pt particles (considering the small amount of deposited Pt material, the nature of the sputtering process, and the roughness of the CdS:Cu film surface, the Pt was presumably in the form of nanoparticles although the particles were too small to be observed in SEM) deposited onto the photocathode surface, the transient photocurrents became negligible (Figure 5a). While SEM imaging does not have the required resolution to see the Pt nanoparticles, in principle, X-ray photoelectron spectroscopy (XPS) can elucidate the oxidation state of platinum and provide valuable information on the mass loading of platinum at the surface. Although the remnant of photocurrent (the ratio of the photocurrent density at the end of the last light cycle to that at the end of the first light cycle) after the current−time stability test for 20 min of the bare CdS:Cu (17%) was larger than that of the bare Cu_2O (0%),[15] it was still too low for practical application. However, the remnant of photocurrent of the photocathode was increased to 98% after the deposition of the Pt cocatalyst. This stability of the CdS:Cu/Pt photocathode was significantly better than that of the Cu_2O protected by ZnO:Al/TiO_2/Pt, for which a remnant of 78% was obtained after 20 min stability test under similar scavenger-free condition, possibly due to a self-photoreduction of the photocathode as reported by Grätzel's group.[15] The photocorrosion prevention role of cocatalyst was also pointed out by Domen et al. for their observed stability enhancement for the Ta_3N_5 photoanode with oxygen evolving Co-Pi cocatalyst.[41] In fact, Pt was found to be a good catalyst to facilitate the transfer of electrons from the photocathode to water by reducing the overpotential of the water reduction reaction.[42] As a result, the accumulation of electrons at the photocathode/electrolyte interface was greatly reduced to avoid the photocathode self-reduction. Figure 5b, comparing the current−potential behaviors of CdS:Cu and CdS:Cu/Pt, revealed that the surface modification on the photocathode by Pt particles not only enhanced the photocurrent but also positively shifted the onset potential of the cathodic photocurrent by 90 mV, further confirming the important role of the Pt cocatalyst.[43]

The photoelectrochemical reduction of water into hydrogen by using the CdS:Cu (@5.4%)/Pt photocathode was carried out at 0 V versus RHE in 1.0 M Na_2SO_4 electrolyte under simulated AM 1.5 illumination. While the dashed black line in Figure 5c corresponds to the ideal hydrogen production calculated from the photocurrent passing through the photoelectrode, the solid red line represents the actual hydrogen production and the solid blue line represents the nearly stoichiometric amount of oxygen production. The control experiments in the dark at the same potential did not produce any detectable hydrogen and oxygen. The Faradic efficiency of hydrogen production was calculated to be 73%, which was close to that of GaP nanowires,[11] illustrating that most of the photoinduced electrons produced in the photocathode participated in reducing water into hydrogen.[44] Although it is difficult to quantitatively compare the performance of the CdS:Cu/Pt photocathode with others as a result of large variations of measurement conditions, we could consider those characterized in similar nearly neutral scavenger-free electrolyte, which is important in the practical large-scale application. The photocathode reported here showed larger photocurrent even than those with narrower band gaps, such as $CuNb_3O_8$ (1.5 eV), $CaFe_2O_4$ (1.9 eV), and GaP (2.2 eV) both in planar and nanowire form.[11,44,45] To compare with available stability data, CdS:Cu/Pt photocathode also exhibited better stability than Cu_2O (2.0 eV) and InP (1.3 eV) under comparable

dx.doi.org/10.1021/jp410242e | J. Phys. Chem. C 2014, 118, 2306−2311

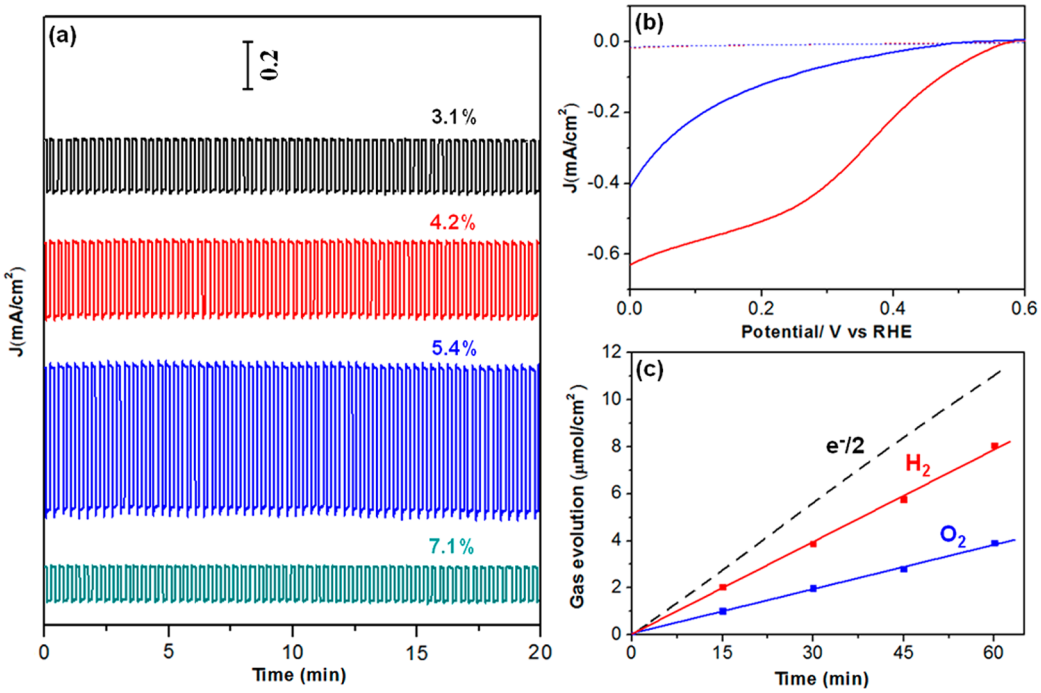

Figure 5. (a) Current−time measurements for a number of CdS:Cu/Pt photocathodes with different Cu concentrations held at 0 V versus RHE in 1.0 M Na_2SO_4 electrolyte at pH 9 under chopped simulated AM 1.5 light. The insert is the 0.2 mA/cm^2 scale bar. (b) Current−potential behaviors for photoelectrode of CdS:Cu (@5.4%) (blue line) and CdS:Cu (@5.4%)/Pt (red line), respectively. The solid lines were measured under simulated AM 1.5 light while the dotted lines were in the dark. (c) Evolution of hydrogen (red line) over CdS:Cu (@5.4%)/Pt at 0 V versus RHE in 1.0 M Na_2SO_4 electrolyte under simulated AM 1.5 illumination. Evolution of oxygen (blue line) over the counter electrode is plotted for comparison. The dashed black line shows ideal hydrogen evolution assuming a Faradic efficiency of 100%.

conditions.[9,15] Compared with the theoretical photocurrent density of 7.2 mA/cm^2 determined by the CdS band gap, the value of our CdS:Cu/Pt photocathode (0.6 mA/cm^2 as shown in Figure 5a) and the corresponding quantum efficiency at present were low. However, it is expected that with more effort and further optimization including crystalline quality, surface/volume ratio, doping, and cocatalyst deposition, p-type CdS based photocathode, with its visible light response, appropriate energetics for water redox reactions, and high photocorrosion durability,[46] may become an important photoelectrode for energy production.

CONCLUSIONS

In summary, we have successfully fabricated an hexagonal-structured p-type Cu-doped CdS thin film with a direct band gap of 2.37 eV and a high surface-to-volume ratio. The bare CdS:Cu photocathode was found to possess a large transient photocurrent and low stability. However, these problems were successfully eliminated through modifying the photocathode surface with Pt cocatalyst, which could effectively reduce the overpotential of water reduction and thus reduce the accumulation of electrons at the photocathode/electrolyte interface. The Pt modification further enhanced the photocurrent and positively shifted the onset potential of the cathodic photocurrent by 90 mV. Our observation of hydrogen evolution from the p-type CdS:Cu/Pt photocathode in the nearly neutral and scavenger-free electrolyte demonstrated for the first time the feasibility of using a p-type CdS-based photocathode to achieve hydrogen production.

AUTHOR INFORMATION

Corresponding Author

*E-mail: xdxiao@phy.cuhk.edu.hk. Tel: (852) 3943-4388. Fax: (852) 2603-5204.

Notes

The authors declare no competing financial interest.

ACKNOWLEDGMENTS

This work was supported by the CUHK Focused Scheme B Grant "Center for Solar Energy Research", the GRF of HKSAR (Project No. 414710), and the National Major Science Research Program of China (Project No. 2012CB933700). The authors thank Prof. Jimmy C. Yu and Mr. Ting Gu for their help in hydrogen evolution detection and Dr. Shihang Yang for the Mo thin film preparation.

REFERENCES

(1) Krol, R. D.; Grätzel, M. *Photoelectrochemical Hydrogen Production*; Springer: New York, NY, 2012.

(2) Khaselev, O.; Turner, J. A. A Monolithic Photovoltaic-Photoelectrochemical Device for Hydrogen Production via Water Splitting. *Science* **1998**, *280*, 425−427.

(3) Reece, S. Y.; Hamel, J. A.; Sung, K.; Jarvi, T. D.; Esswein, A. J.; Pijpers, J. H.; Nocera, D. G. Wireless Solar Water Splitting Using Silicon-Based Semiconductors and Earth-Abundant Catalysts. *Science* **2011**, *334*, 645−648.

(4) Faunce, T. A.; Lubitz, W.; Rutherford, A. W.; MacFarlane, D.; Moore, G. F.; Yang, P. D.; Nocera, D. G.; Moore, T. A.; Gregory, D. H.; Fukuzumi, S.; et al. Energy and Environment Policy Case for a Global Project on Artificial Photosynthesis. *Energy Environ. Sci.* **2013**, *6*, 695−698.

(5) Fujishima, A.; Honda, K. Electrochemical Photolysis of Water at a Semiconductor Electrode. *Nature* **1972**, *238*, 37−38.

(6) Wagner, F. T.; Somorjai, G. A. Photocatalytic Hydrogen Production from Water on Pt-Free $SrTiO_3$ in Alkali Hydroxide Solutions. *Nature* **1980**, *285*, 559−560.
(7) Kudo, A.; Miseki, Y. Heterogeneous Photocatalyst Materials for Water Splitting. *Chem. Soc. Rev.* **2009**, *38*, 253−278.
(8) Boettcher, S. W.; Spurgeon, J. M.; Putnam, M. C.; Warren, E. L.; Turner-Evans, D. B.; Kelzenberg, M. D.; Maiolo, J. R.; Atwater, H. A.; Lewis, N. S. Enegy-Conversion Properties of Vapor-Liquid-Solid-Grown Silicon Wire-Array Photocathodes. *Science* **2010**, *327*, 185−187.
(9) Khaselev, O.; Turner, J. A. Electrochemical Stability of p-$GaInP_2$ in Aqueous Electrolytes toward Photoelectrochemical Water Splitting. *J. Electrochem. Soc.* **1998**, *145*, 3335−3339.
(10) Lee, M. H.; Taki, K.; Zhang, J.; Kapadia, R.; Zheng, M.; Chen, Y. Z.; Nah, J.; Matthews, T. S.; Chueh, Y. L.; Ager, J. W.; et al. p-Type InP Nanopillar Photocathodes for Efficient Solar-Driven Hydrogen Production. *Angew. Chem., Int. Ed.* **2012**, *51*, 10760−10764.
(11) Liu, C.; Sun, J. W.; Tang, J. Y.; Yang, P. D. Zn-Doped p-Type Gallium Phosphide Nanowire Photocathodes from a Surfactant-Free Solution Synthesis. *Nano Lett.* **2012**, *12*, 5407−5411.
(12) Hisatomi, T.; Dotan, H.; Stefik, M.; Sivula, K.; Rothschild, A.; Grätzel, M.; Mathews, N. Enhancement in the Prerfomance of Ultrathin Hematite Photoanode for Water Splitting by an Oxide Underlayer. *Adv. Mater.* **2012**, *24*, 2699−2702.
(13) Su, J.; Feng, X.; Sloppy, J. D.; Guo, L.; Grimes, C. A. Vertically Aligned WO_3 Nanowire Arrays Grown Directly on Transparent Conducting Oxide Coated Glass: Synthesis and Photoelectrochemical Properties. *Nano Lett.* **2011**, *11*, 203−208.
(14) Huang, Q.; Kang, F.; Liu, H.; Li, Q.; Xiao, X. D. Highly Aligned $Cu_2O/CuO/TiO_2$ Core/Shell Nanowire Arrays as Photocathodes for Water Photoelectrolysis. *J. Mater. Chem. A* **2013**, *1*, 2418−2425.
(15) Paracchino, A.; Laporte, V.; Sivula, K.; Grätzel, M.; Thimsen, E. Highly Active Oxide Photocathode for Photoelectrochemical Water Reduction. *Nat. Mater.* **2011**, *10*, 456−461.
(16) Grätzel, M. Photoelectrochemical Cells. *Nature* **2001**, *414*, 338−344.
(17) Walter, M. G.; Warren, E. L.; Mckone, J. R.; Boettcher, S. W.; Mi, Q.; Santori, E. A.; Lewis, N. S. Solar Water Splitting Cells. *Chem. Rev.* **2010**, *110*, 6446−6473.
(18) Shangguan, W. F.; Yoshida, A. Photocatalytic Hydrogen Evolution from Water on Nanocomposites Incorporating Cadmium Sulfide into the Interlayer. *J. Phys. Chem. B* **2002**, *106*, 12227−12230.
(19) Walukiewicz, W. Intrinsic Limitations to the Doping of Wide-Gap Semiconductors. *Phys. B* **2001**, *302*−*303*, 123−134.
(20) Sathich, M.; Viswanathan, B.; Viswanath, R. P. Alternate Synthetic Strategy for the Preparation of CdS Nanoparticles and Its Exploitation for Water Splitting. *Int. J. Hydrogen Energy* **2006**, *31*, 891−898.
(21) Kanan, M. W.; Nocera, D. G. In Situ Formation of an Oxygen-Evolving Catalyst in Neutral Water Containing Phosphate and Co^{2+}. *Science* **2008**, *321*, 1072−1075.
(22) Desnica, U. V. Doping Limits in II-VI Compounds-Challenges, Problems and Solutions. *Prog. Cryst. Growth Charact. Mater.* **1998**, *36*, 291−357.
(23) Grimes, C. A.; Varghese, O. K.; Ranjan, S. *Light, Water, Hydrogen: The Solar Generation of Hydrogen by Water Photoelectrolysis*; Springer: New York, NY, 2008.
(24) Shiraki, Y.; Shimada, T.; Komatsubara, K. F. Ion Implantation of Nitrogen into Cadmium Sulfide. *J. Appl. Phys.* **1972**, *43*, 710−718.
(25) Anderson, W. W.; Mitchell, J. T. Phosphorous-Ion-Implanted CdS. *Appl. Phys. Lett.* **1968**, *12*, 334−336.
(26) Kashiwaba, Y.; Kanno, I.; Ikeda, T. p-Type Characteristics of Cu-Doped CdS Thin Films. *Jpn. J. Appl. Phys.* **1992**, *31*, 1170−1175.
(27) Kashiwaba, Y.; Komatsu, T.; Nishikawa, M.; Ishikawa, Y.; Segawa, K.; Hayasi, Y. X-Ray Diffraction Studies of p-CdS:Cu Thin Films. *Thin Solid Films* **2002**, *408*, 43−50.
(28) Ullrich, B.; Ezumi, H.; Keitoku, S.; Kobayashi, T. Luminescence Properties of p-Type Thin CdS Films Prepared by Laser Ablation. *Mater. Sci. Eng.* **1995**, *B35*, 117−159.
(29) Sebastian, P. J. p-Type CdS Thin Films Formed by in Situ Cu Doping in the Chemical Bath. *Appl. Phys. Lett.* **1993**, *23*, 2956−2958.
(30) Kashiwaba, Y.; Isojima, K.; Ohta, K. Improvement in the Efficiency of Cu Doped CdS/Non-Doped CdS Photovoltaic Cells Fabricated by an All-Vacuum Process. *Sol. Energy Mater. Sol. Cells* **2003**, *75*, 253−259.
(31) Juan, M. T.; Arturo, M. A.; Mauricio, O. L. Electrical Characterization of Al, Ag and In Contacts on $CuInS_2$ Thin Films Deposited by Spray Pyrolysis. *Sol. Energy Mater. Sol. Cells* **2009**, *93*, 544−548.
(32) Fernandez, A. M.; Dheree, N.; Turner, J. A.; Martinez, A. M.; Arriaga, L. G.; Cano, U. Photoelectrochemical Characterization of the $Cu(In,Ga)S_2$ Thin Film Prepared by Evaporation. *Sol. Energy Mater. Sol. Cells* **2005**, *85*, 251−259.
(33) Nishidate, K.; Sato, T.; Matsukura, Y.; Baba, M.; Hasegawa, M.; Sasaki, T. Density-Functional Electronic Structure Calculations for Native Defects and Cu Impurities in CdS. *Phys. Rev. B* **2006**, *74*, 035210.
(34) Yu, J. C.; Wu, L.; Lin, J.; Li, P. S.; Li, Q. Microemulsion-Mediated Solvothermal Synthesis of Nanosized CdS-Sensitized TiO_2 Crystalline Photocatalyst. *Chem. Commun.* **2003**, *13*, 1552−1553.
(35) Wang, X. N.; Zhu, H. J.; Xu, Y. M.; Wang, H.; Tao, Y.; Hark, S. K.; Xiao, X. D.; Li, Q. Aligned ZnO/CdTe Core-Shell Nanocable Arrays on Indium Tin Oxide: Synthesis and Photoelectrochemical Properties. *ACS Nano* **2010**, *4*, 3302−3308.
(36) Wang, X. N.; Wang, J.; Zhou, M. J.; Wang, H.; Xiao, X. D.; Li, Q. CdTe Nanorods Formation via Nanoparticle Self-Assembly by Thermal Chemistry Method. *J. Cryst. Growth* **2010**, *312*, 2310−2314.
(37) Grus, M.; Sikorska, A. Characterization of the Absorption Edge in Crystalline CdS:Cu Powder by Use of Photoacoustic and Reflection Spectroscopy. *Phys. B* **1999**, *266*, 139−145.
(38) Grimmeiss, H. G.; Memming, R. p-n Photovoltaic Effect in Cadmium Sulfide. *J. Appl. Phys.* **1962**, *33*, 2217−2222.
(39) Murai, H.; Abe, T.; Matsuda, J.; Sato, H.; Chiba, S.; Kashiwaba, Y. Improvement in the Light Emission Characteristics of CdS:Cu/CdS Diodes. *Appl. Surf. Sci.* **2005**, *244*, 351−354.
(40) Woods, J.; Champion, J. A. Hole Conduction and Photovoltaic Effects in CdS. *J. Electron. Control* **1959**, *7*, 243−253.
(41) Li, Y. B.; Takata, T.; Cha, D.; Takanabe, K.; Minegishi, T.; Kubota, J.; Domen, K. Vertically Aligned Ta_3N_5 Nanorod Arrays for Solar-Driven Photoelectrochemical Water Splitting. *Adv. Mater.* **2013**, *25*, 125−131.
(42) Baba, R.; Nakabayashi, S.; Fujishima, A. Investigation of the Mechanism of Hydrogen Evolution during Photocatalytic Water Decomposition on Metal-Loaded Semiconductor Powders. *J. Phys. Chem.* **1985**, *89*, 1902−1905.
(43) Mckone, J. R.; Pieterick, A. P.; Gray, H. B.; Lewis, N. S. Hydrogen Evolution from Pt/Ru-Coated p-Type WSe_2 Photocathodes. *J. Am. Chem. Soc.* **2013**, *135*, 223−231.
(44) Joshi, U. A.; Maggard, P. A. $CuNb_3O_8$: A p-Type Semiconducting Metal Oxide Photoelectrode. *J. Phys. Chem. Lett.* **2012**, *3*, 1577−1581.
(45) Cao, J.; Kako, T.; Li, P.; Ouyang, S.; Ye, J. Fabrication of p-Type $CaFe_2O_4$ Nanofilms for Photoelectrochemical Hydrogen Generation. *Electronchem. Commun.* **2011**, *13*, 275−278.
(46) Vayssieres, L. *On Solar Hydrogen & Nanotechnology*; John Wiley: Singapore, 2009.